Journal of Alloys and Compounds 509 (2011) 2289–2293

Contents lists available at ScienceDirect

Journal of Alloys and Compounds

journal homepage: www.elsevier.com/locate/jallcom

Phase separation and formation of core-type microstructure of Al–65.5 mass% Bi immiscible alloys

R. Dai, S.G. Zhang*, Y.B. Li, X. Guo, J.G. Li

School of Materials Science and Engineering, Shanghai Jiao Tong University, 800 Dong Chuan Rd., Shanghai 200240, PR China

ARTICLE INFO

Article history:
Received 3 September 2010
Received in revised form 22 October 2010
Accepted 30 October 2010
Available online 10 November 2010

Keywords:
Metals and alloys
Microstructure
Composite materials
Precipitation

ABSTRACT

Core-type microstructures offer a unique combination of properties of both layers. Phase separation and formation of core-type microstructure in Al–65.5 mass% Bi hyper-monotectic alloys were studied by melting in quartz crucibles with orifices at the bottom and then ejecting the melt into silicon oil. Effects of processing parameters were investigated by changing the free fall distance of droplets and the temperature of silicon oil where the droplets solidified. Based on ANSYS simulation, the cooling rate and temperature gradient of droplets were estimated. As the free fall distance and silicon oil temperature decrease, both the temperature gradient and cooling rate tend to increase, leading to great changes in Marangoni and Stokes motions, and hence causing the transitions of morphology between a crescent-shape shell and a regular shell. The solidification paths under different processing parameters were analyzed, and it was concluded and exemplified that only if the effects of Marangoni and Stokes are discreetly balanced can the regular core-type particles be obtained.

1. Introduction

Immiscible alloys have attracted much attention due to their unique combination of properties, for example, Al–Bi and Al–Pb alloys can offer excellent self-lubricant property due to existence of soft Bi or Pb particles in the hard matrix [1]. Many studies have been carried out on the solidification of immiscible alloys [2–4]. It was found that this kind of alloy easily suffers from serious segregation during ordinary solidification process. Once the homogeneous liquid cools into the miscibility gap, two liquid phases which have different compositions coexist in equilibrium. The globules of minority liquid will be generated, and then grow and migrate under a combined effect arising from many factors, including the Marangoni motion [5,6], Brownian motion [7], convective flow [8], gravity level [9], wettability between the two liquid phases [10], cooling rate [11] and so on. As a result, an immiscible liquid usually solidifies into two layers at normal ground conditions, which has restricted its broad applications.

Nevertheless, by tailoring the processing conditions, the characteristics of rapid spatial phase separation during solidification of immiscible alloys provide a distinctive opportunity to in situ fabricate core-type composites. Recently, Wang et al. [12] and Ohnuma et al. [13] reported core-type Cu–Sn–Bi immiscible alloy powders prepared by gas atomization. This kind of Cu cored/Sn–Bi shelled alloy powders has great potential in electronic applications owing to the combination of superior electric and thermal conductivities of the core and lead-free solder of the shell. Al is comparable to Cu in electric and thermal conductivities, but is only one-third of the density of Cu, which will bring significant weight lightening effect. However, relevant work on Al-cored particles has rarely been reported. Zhang and Xian [14] showed that Sn tends to locate with Bi when added to Al–10.7% Bi (number indicates mass%, hereinafter) monotectic alloy. Considering this, the formation of core-type morphology in Al–Bi binary alloys is essential to fabricate the Al-cored/Sn–Bi-shelled particles. In this paper, effects of processing parameters on core-type Al–65.5% Bi hyper-monotectic alloys were investigated by changing the free fall distance of droplets and the temperature of silicon oil where the droplets solidified. The cooling rate and temperature gradient of droplets were estimated by ANSYS simulation. The influencing mechanism of the processing parameters was analyzed, and how to get regular core-type Al–65.5% Bi alloy particles was discussed and exemplified.

2. Experimental procedure

Pure element (99.99% in purity) pieces about 3 g with the nominal composition of Al–65.5% Bi were melted in a quartz crucible by high frequency induction under argon atmosphere. The melt was overheated to 1540 K, which was 230 K above its critical temperature (T_c = 1310 K), for 10 min to ensure sufficient mixing of the components. Then, the homogeneous melt was ejected from the orifice (about 0.8 mm in diameter) at the bottom of crucible into silicon oil beneath the orifice. Three free fall distances of droplets, 75, 100 and 145 mm, were selected to investigate the effect

* Corresponding author. Tel.: +86 21 5474 4246; fax: +86 21 5474 4246.
E-mail addresses: dairongrong@sjtu.edu.cn (R. Dai), sgzhang@sjtu.edu.cn (S.G. Zhang).

0925-8388/$ – see front matter © 2010 Elsevier B.V. All rights reserved.
doi:10.1016/j.jallcom.2010.10.203

on macroscopic morphologies of particles. For studying the influence of silicon temperature, the melt was superheated to 1610 K before it was ejected into silicon oil (30 mm below the orifice) with different temperatures of 283 or 383 K. The temperature of melt was measured by an infrared pyrometer whose surface emissivity was set to be 0.2 calibrated by a thermocouple.

Using a JEOL JSM 6460 scanning electron microscopy (SEM) with energy dispersive spectroscopy (EDS), the phase constitutions and macroscopic morphologies of particles were investigated. The particles were etched using a solution ($HF:HCl:HNO_3:H_2O = 2:3:5:190$) before observation.

3. Results and discussion

More than 70% particles with similar size are alike in morphologies. Fig. 1 shows the typical cross-sectional morphologies of Al–65.5% Bi particles under different free fall distances of droplets. It can be observed that phase separation took place and core-type morphologies were formed. For a short free fall distance of 75 mm, as displayed in Fig. 1a, a white phase encapsulates a black phase. Also seen are a very small white core and some white spots near the center. EDS analysis of the spots marked in Fig. 1d indicates that the white phase is nearly pure Bi (99.1%) while the black phase is pure Al. It is similar for the particles with other sizes that all the dark and white phases contain more than 80% of Al and Bi, respectively. As the free fall distance becomes longer, the white phase tends to coalescence and move to one side, and there are also some "islands" and spots of white phase in the black phase matrix, as shown in Fig. 1b, suggesting a heavy gravitational segregation. With a further increase in the free fall distance to 145 mm, the white shell cannot fully encapsulate the black phase and an irregular crescent-shape-shell microstructure forms (Fig. 1c), showing a more complete phase separation. From Fig. 1, it suggests that a short distance between the orifice and silicon oil favors the formation of relatively regular core-type morphology of Al–65.5% Bi alloy.

Two kinds of temperature of 283 and 383 K were used to examine the effect of temperature of silicon oil on macroscopic morphologies of particles. According to the above results, the distance between the orifice and silicon oil was fixed to 30 mm. As shown in Fig. 2, the phase separation occurred and core-type microstructure emerged, too. With increasing the temperature of silicon oil, the core-type Al–Bi particles have a tendency to form crescent-shape shells.

Marangoni motion and gravity play important roles in phase separation and formation of core-type structure [11,12]. The center of a droplet generally possesses higher temperature and thus lower interfacial energy than the surface. So the liquid globules will move to the center because of Marangoni motion [5,6,15,16]. They also tend to float under buoyant force. The velocity of globules due to Marangoni motion (v_m) and gravity (v_s) can be calculated by Eqs. (1) [6,17] and (2) [17], respectively

$$v_m \approx \frac{-2r}{3(3\mu_d + 2\mu_m)} \cdot \frac{\partial \sigma}{\partial T} \cdot \frac{\partial T}{\partial x} \quad (1)$$

$$v_s \approx \frac{2g\Delta\rho r^2}{3\mu_m} \cdot \frac{\mu_d + \mu_m}{3\mu_d + 2\mu_m} \quad (2)$$

where r is the diameter of the globule; μ_d and μ_m are the viscosities of the globule and matrix, respectively; σ is the interfacial energy; x is the distance; g is the gravity coefficient; $\Delta\rho$ is the difference of density between the globule and matrix.

The temperature gradient in a droplet is difficult to be directly measured during free fall and descending in oil. So, the ANSYS software was applied to simulate the cooling of droplet. For heat transfer, the conduction, convection and radiation processes were considered during free fall of droplets while only the conduction and convection processes were taken into account when droplets descended in oil. The parameters used and the references for computing parameters are listed in Table 1. Density of the alloy is estimated as the sum of the mole fraction times the density of each element. It is rather complex to obtain the temperature profile of the whole cooling process where the diffusion, phase separation, temperature and flow fields are closely coupled. However, the phase separation will be triggered when the melt temperature falls below T_c of 1310 K. We could evaluate the temperature fields of droplets just at this point for comparison. The simulated results of temperature profiles of droplets under various conditions are shown in Fig. 3 when the temperature of the surface of droplet reached T_c. Then the temperature gradient and cooling rate of droplet can be obtained. Fig. 4a shows that the estimated temperature gradient and cooling rate decrease as the free fall distance increases. With increasing the temperature of silicon oil, as seen from Fig. 4b, the temperature gradient also declines, and the cooling rate changes little for the case of melt temperature of 1610 K.

Table 1
The parameters used in the simulation.

Parameters	Values	References
Initial velocity of droplet, m/s	1.0	
Density of droplet, kg/m^3	4100	
Specific heat of droplet, J/(kg K)	730	*
Thermal conductivity of droplet, W/(m K)	52.4	[18,19]
Heat transfer coefficients of air, W/(m^2 K)	134.3206	[20,21]
Heat transfer coefficients of silicon oil, W/(m^2 K)	35067.2	[20,22]
Surface emissivity, ε	0.2	
Stefan-Boltzmann constant, W/(m^2 K^4)	5.67×10^{-8}	

* Neumann–Kopp rule.

Fig. 5 displays the calculated results of v_m and v_s at 1200 K. For example, when $r = 5$ μm, $\partial\sigma/\partial T = 1.39 \times 10^{-4}$ J/(m^2 K) [16], μ_d and μ_m are estimated from [23], v_m of Al globules dispersed in liquid Bi is 8 mm/s, which is 16 times as fast as v_s (0.5 mm/s) for a temperature gradient of 80 K/mm. But in the case of a larger temperature gradient of 300 K/mm comparable to those shown in Fig. 4a, v_m will be 62 times the value of v_s. On the other hand, from Eqs. (1) and (2), it is obviously seen that v_m is proportional to r whereas v_s scales with r^2, implying that v_s increases much quicker with r than v_m. For example, when the size of globules increases from 5 to 283 μm under the same temperature gradient (300 K/mm), v_s will begin to exceed v_m. This suggests Marangoni motion plays a critical role at the early state of phase separation, and with the proceeding of cooling, the temperature gradient decreases and size of globules increases, the effect of gravity will become more and more pronounced accordingly. Evidently, the time that is allowed by cooling rate for keeping liquid states is an important factor to determine the effect of gravity.

According to Fig. 4, both the temperature gradient and cooling rate are highest for the free fall distance of 75 mm, resulting in the formation of relatively complete core–shell morphology due to large v_m and scarce time for gravitational sedimentation. It is also confirmed by the presence of a small Bi-core which may be formed by the coagulation of lately formed liquid globules of Bi in supersaturated Al-rich matrix nearby the center, but are unable to move to the outside layer of Bi in a limited solidification time. With increasing the free fall distance to 100 mm, both the temperature gradient and cooling rate get shallower, leading to a slower v_m and longer time for sedimentation as well as for local agglomeration of lately formed liquid globules. Further increase in the free fall distance gives rise to a more faint Marangoni effect but a more sufficient time for migration and coagulation of liquid spheres, and hence a nearly complete segregated microstructure with fewer spheres trapped within will be produced, where the lighter Al phase floats upwards because of the relatively larger effect of gravity. This can be clearly seen in Fig. 1.

Therefore, the possible solidification paths during solidification of Al–65.5% Bi alloys could be illustrated in Fig. 6. The sketch on the

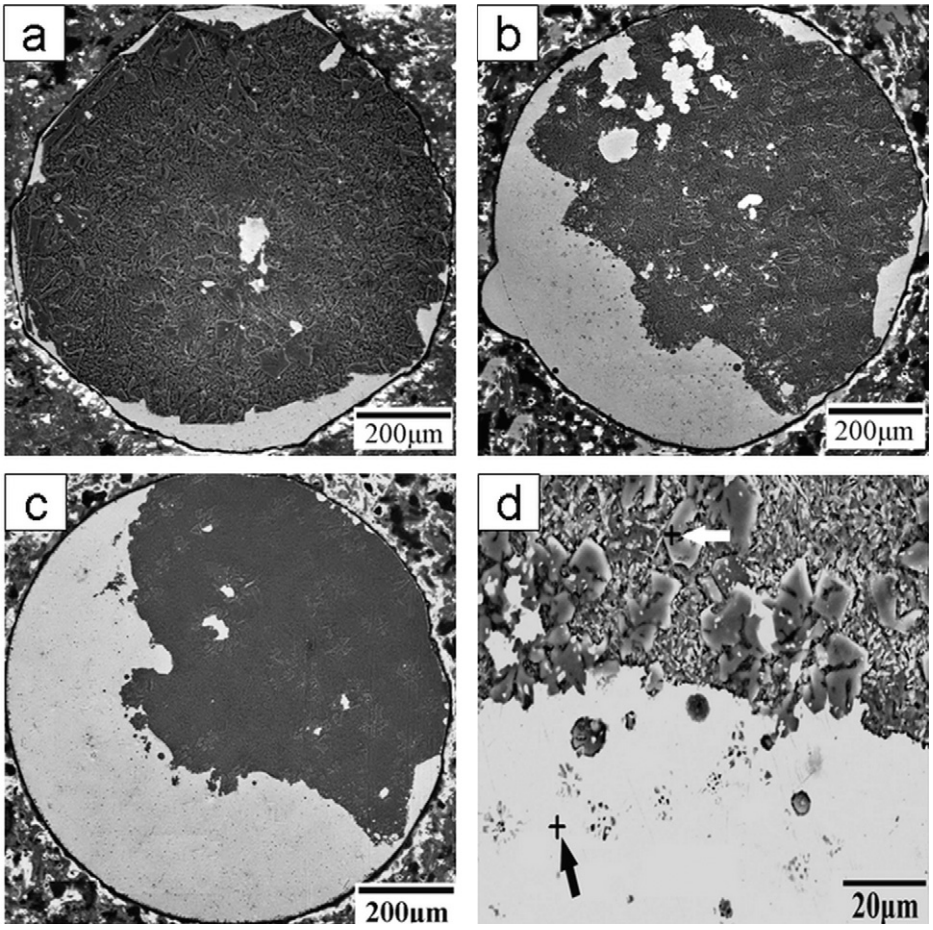

Fig. 1. Cross-sectional morphologies of Al–65.5 mass% Bi particles produced under the temperature of melt of 1540 K, the temperature of silicon oil of 283 K and the free fall distance of (a) 75 mm, (b) 100 mm, and (c) 145 mm. The spots for EDS analysis are marked by arrows in (d) which is a magnified micrograph of (c).

left represents a schematic diagram of miscibility gap in Al–Bi alloy. Generally, much lower driving force is needed for liquid–liquid transition than that for liquid–solid transition, particularly very little is for a composition with highest critical point [1,24], such as Al–65.5% Bi alloy. When the homogeneous melt is undercooled across the critical temperature to point "a", it readily separates into the corresponding compositions along the binodal boundary, that is, the primary liquid phase separation occurs. Notwithstanding this, the surface segregation of Bi still most probably takes place before the primary bulk liquid phase separation, because Bi has lower surface tension than Al. We have found that the surface of Al–Bi particles is always covered by more or less a layer of Bi irrespective of compositions [15]. Similar facts also exist in Al–Pb powders encased a layer of Pb [25], and Fe–Sn particles with Sn shells [26]. Furthermore, the simulations carried out by Qin et al. [26] and Luo et al. [27] have confirmed that a very thin layer of

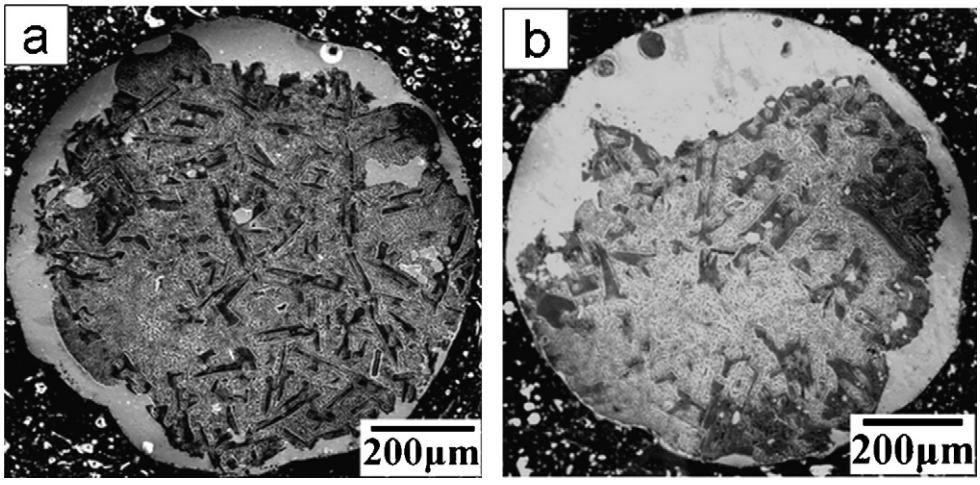

Fig. 2. Cross-sectional morphologies of Al–65.5 mass% Bi particles produced under the temperature of melt of 1610 K, the free fall distance of 30 mm and the temperature of silicon oil of (a) 283 K and (b) 383 K.

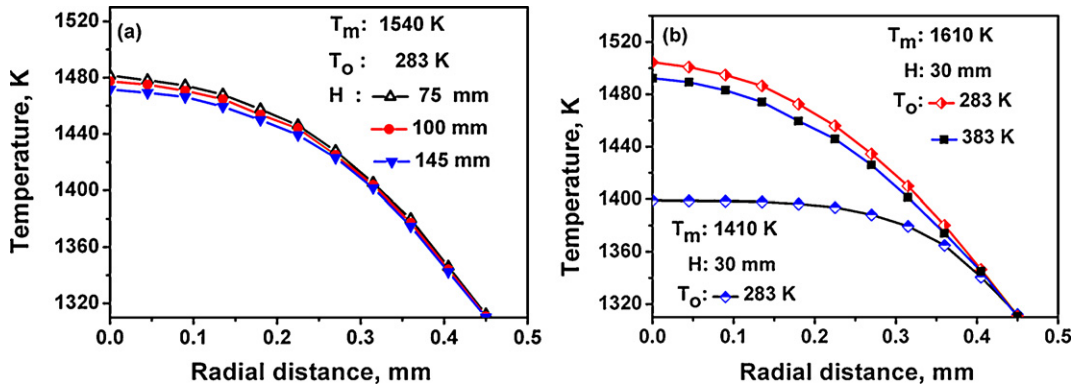

Fig. 3. Simulated temperature profiles in Al–65.5 mass% Bi droplets for (a) different free fall distances and (b) different temperatures of silicon oil and melt.

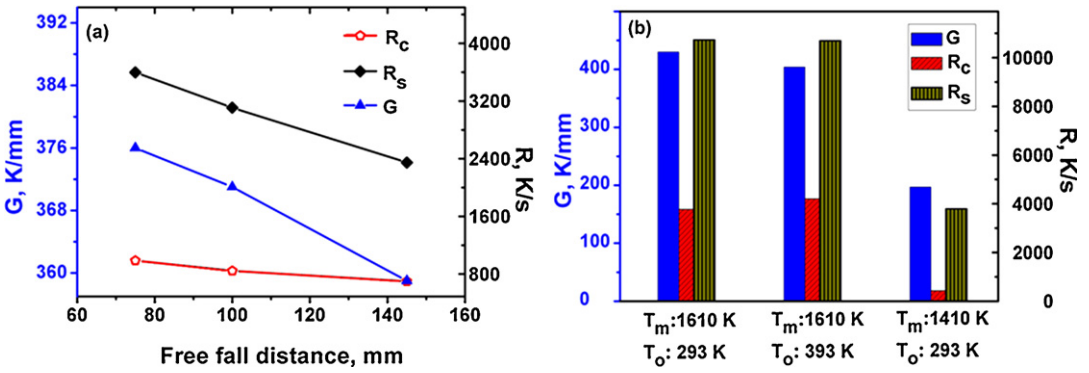

Fig. 4. Estimated temperature gradient (G), cooling rate of the center (R_c) and surface (R_s) in Al–65.5 mass% Bi droplets for (a) different free fall distances and (b) different temperatures of silicon oil and melt.

surface segregation forms rapidly before the decomposition of bulk liquid phase. Once the Bi-rich thin layer is formed, a neighboring layer depleted in Bi emerges, and thus a concentrate fluctuation along the radial direction of droplet will be produced. Following this, the liquid globules of Al will be generated where the supersaturation reaches a critical value of that temperature, as represented by microstructure (a) on the right of Fig. 6.

The growth of liquid globules depends mainly on Ostwald ripening at the very beginning, and then on Brownian and Marangoni motions [1]. Despite Stokes motion will weigh gradually heavier with the snowball-like growth of globules, it is still quite weightless due to small size of "snowballs", which is confirmed by the above calculations of ν_m and ν_s. So, the liquid globules of Al will move to the center of droplet under the effect of Marangoni, and will grow further by diffusion and coagulate during movement, as shown by the schematic microstructure (b) in Fig. 6. In the end,

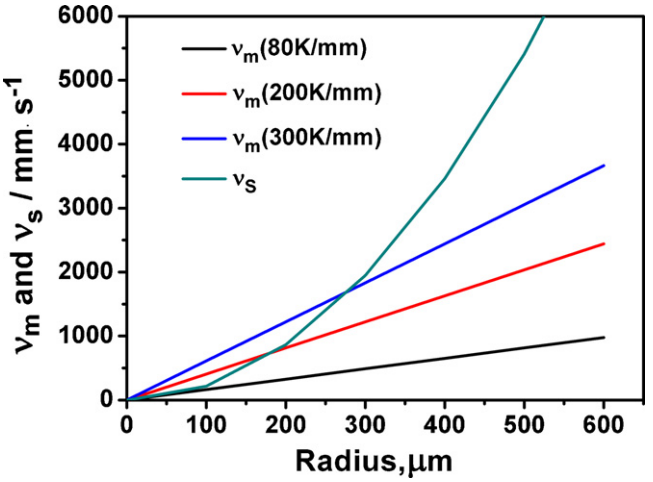

Fig. 5. Calculated ν_m and ν_s as a function of radius of the liquid Al globules inside Al–65.5 mass% Bi droplets at 1200 K.

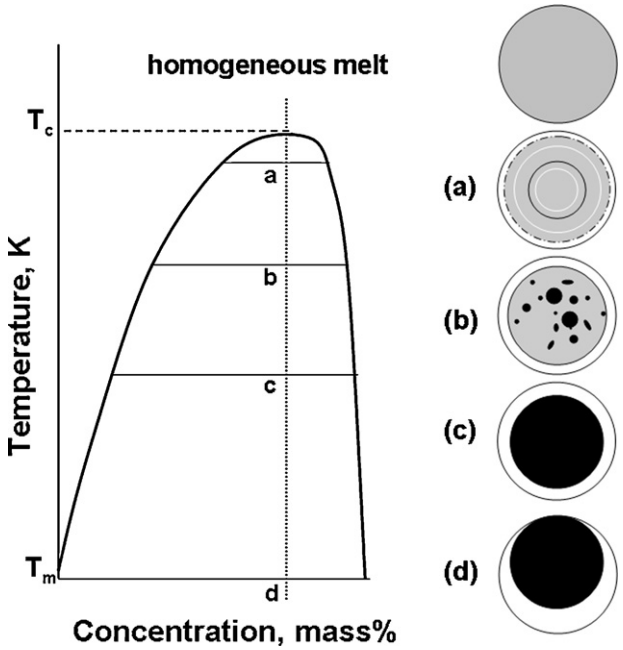

Fig. 6. Schematic representation of phase separation and formation of core-type microstructure during cooling of an immiscible liquid.

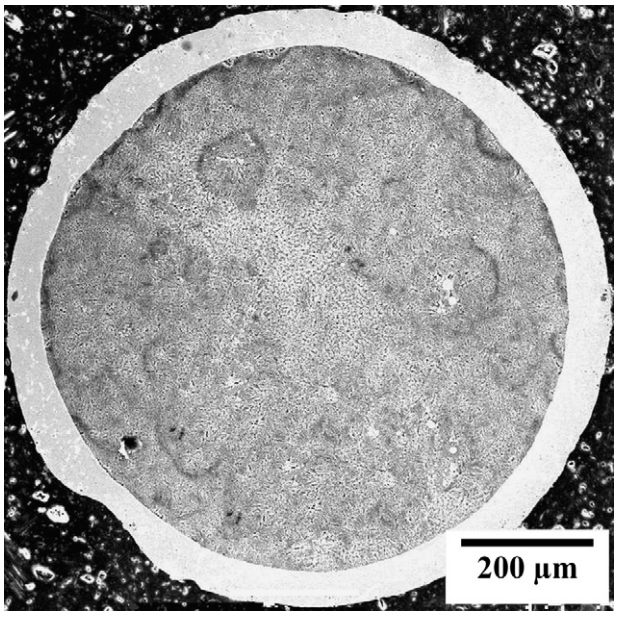

Fig. 7. Cross-sectional morphology of a regular core-type Al–65.5 mass% Bi particle produced under the temperature of silicon oil of 283 K, free fall distance of 30 mm and temperature of melt of 1410 K.

these spheres will assemble at the center and form a core, as illustrated by microstructure (c). If the droplet still retains in liquid state at this time, the core tends to move away from the center to form a crescent-shape-shell type structure, as shown by microstructure (d) in Fig. 6. That is because ν_s usually exceeded ν_m for such a "big" core, along with a faded temperature gradient on cooling. Additionally, once the supersaturation degree becomes high enough during cooling process, the Al phase could nucleate repeatedly in Bi-rich liquid and vice versa. But when temperature is low and viscosity is high, these lately formed liquid globules may have no time to completely coalesce and migrate, and they would be trapped locally by solidification in the form of irregular "block", spot or even film confined within interdendritic zones and also some fine particles of various sizes dispersed in matrix, which can be clearly seen in Fig. 1.

It is worth pointing out that spinodal decomposition is also possible for a composition in the center of the miscibility gap. Wang et al. got such kind of microstructure in 52Cu–44Fe–4V alloys [11]. However, irregular microstructure resulted from spinodal decomposition have not been found yet in our experiments. This suggests that liquid phase separation is rather complex depending on many processing conditions and may differ greatly for different systems. The microstructure in the early state of phase separation is not necessarily the same type as is found in the final stage, which may change radically under the effects of diffusion and Marangoni, etc. A simulation on Fe–50 at.% Cu alloy by Qin et al. [26] may support this hypothesis. It can be seen from their modeling that, if time permitted, the spinodal decomposed microstructure will be evolved into a core-type one at last.

From the above discussions, it is very important to obtain regular core–shell morphology through a fine balance between temperature gradient and cooling rate. Indeed, we have successfully got perfect core-type Al–65.5% Bi particles under the conditions of free fall distance of 30 mm, temperature of silicon oil of 283 K and temperature of melt of 1410 K, as shown in Fig. 7. The temperature field, estimated temperature gradient and cooling rate have also been plotted into Figs. 3b and 4b. From Fig. 4b, this case seems to have provided an appropriate temperature gradient and cooling rate (which are moderate compared with the others) so that a good core-type microstructure was formed. So, further study should be focused on quantitatively evaluation of the interplay between temperature gradient and cooling rate to gain regular core-type morphology of immiscible alloys.

4. Conclusions

For Al–65.5% Bi hyper-monotectic alloy solidified under different conditions, the phase separation occurred and the core-type microstructure with an Al-rich core encased by a Bi-rich phase was formed. From the ANSYS simulation, the cooling rate and temperature gradient of droplets solidified under different conditions can be estimated and then velocities of Marangoni and Stokes motions were calculated. It reveals that the temperature gradient and cooling rate should make a compromise to obtain perfect core-type morphology; otherwise, a crescent-shape-shell type would be formed instead. By tuning the processing conditions to free fall distance of 30 mm, temperature of silicon oil of 283 K and temperature of melt of 1410 K, perfect annular shape Al–65.5% Bi alloy has successfully been gotten.

Acknowledgements

This work was financially supported by Shanghai Municipal Science and Technology Committee-Applied Materials Co. Ltd. Joint Foundation (No. 08520740400). Thanks also go to the undergraduate students C.K. Zhao, X. Yang and C. Xiao for their participation.

References

[1] L. Ratke, S. Diefenbach, Mater. Sci. Eng. R15 (1995) 263–347.
[2] Y.J. Liu, D. Liang, J. Alloys Compd. 403 (2005) 110–117.
[3] D. Mirkovic, J. Grobner, R. Schmid-Fetzer, Acta Mater. 56 (2008) 5214–5222.
[4] Y.Z. Chen, F. Liu, G.C. Yang, X.Q. Xu, Y.H. Zhou, J. Alloys Compd. 427 (2007) L1–L5.
[5] C. Marangoni, Ann. Phys. Chem. 143 (1871) 337–354.
[6] N.O. Young, J.S. Goldstein, M.J. Block, J. Fluid Mech. 6 (1959) 350–356.
[7] J.Z. Zhao, Mater. Sci. Eng. A 454–455 (2007) 637–640.
[8] H.L. Li, J.Z. Zhao, Q.X. Zhang, J. He, Metall. Mater. Trans. A 39 (2008) 3308–3316.
[9] A.P. Silva, J.E. Spinelli, A. Garcia, J. Alloys Compd. 480 (2009) 485–493.
[10] G. Wilde, J.H. Perepezko, Acta Mater. 47 (1999) 3009–3021.
[11] C.P. Wang, X.J. Liu, Y. Takaku, I. Ohnuma, R. Kainuma, K. Ishida, Metall. Mater. Trans. A 35 (2004) 1243–1253.
[12] C.P. Wang, X.J. Liu, I. Ohnuma, R. Kainuma, K. Ishida, Science 297 (2002) 990–993.
[13] I. Ohnuma, T. Saegusa, Y. Takaku, C.P. Wang, X.J. Liu, R. Kainumu, K. Ishida, J. Electron. Mater. 38 (2009) 2–9.
[14] H.W. Zhang, A.P. Xian, Acta Metall. Sin. 36 (2000) 347–350.
[15] R. Dai, S.G. Zhang, X. Guo, J.G. Li, Mater. Lett. 65 (2011) 322–325.
[16] I. Kaban, J. Gröbner, W. Hoyer, R. Schmid-Fetzer, J. Mater. Sci. 45 (2010) 2030–2034.
[17] L. Ratke, P.W. Voorhees, Growth and Coarsening, Springer-Verlag, New York, 2002.
[18] R.H. Davis, Int. J. Thermophys. 7 (1986) 609–620.
[19] http://environmentalchemistry.com/yogi/periodic/thermal.html (accessed on-line 7.7.2010).
[20] F.M. White, Viscous Fluid Flow, McGraw-Hill, New York, 1974.
[21] H.Y. Wang, R.P. Liu, Z.J. Zhan, L.L. Sun, W.K. Wang, Acta Metall. Sin. 41 (2005) 940–946.
[22] S. Wakitani, J. Phys.: Conf. Ser. 64 (2007) 012006.
[23] M. Hirai, ISIJ Int. 33 (1993) 251–258.
[24] J.W. Cahn, Met. Trans. 10 A (1979) 119–121.
[25] J.Z. Zhao, Scripta Mater. 54 (2006) 247–250.
[26] T. Qin, H.P. Wang, B. Wei, China Sci. Ser. G 37 (2007) 409–416.
[27] B.C. Luo, X.R. Liu, B. Wei, J. Appl. Phys. 106 (2009) 053523.